Novel Optical Phase Demodulator Based on a Sampling Phase-Locked Loop

Darko Zibar, Leif A. Johansson, *Member, IEEE*, Hsu-Feng Chou, *Member, IEEE*, Anand Ramaswamy, Mark Rodwell, *Fellow, IEEE*, and John E. Bowers, *Fellow, IEEE*

***Abstract*—A novel phase-locked coherent demodulator, based on a sampling phase-locked loop, is presented and investigated theoretically. The demodulator is capable of operating at high frequencies, by using optical sampling to downconvert the high-frequency input radio-frequency signal to the frequency range of the baseband loop. We develop a detailed theoretical model of the (sampling) phase-locked coherent demodulator and perform detailed numerical simulations. The simulation results show that the operation of the sampling demodulator resembles the operation of the baseband demodulator for very short optical pulses (<2 ps). Furthermore, we investigate how the signal-to-noise ratio of the demodulator is affected by timing and amplitude jitter of the pulsed optical source.**

***Index Terms*—Analog links, coherent, microwave photonics, modulators, phase-locked loop (PLL), phase-modulation, sampling.**

I. Introduction

THE use of analog optical links for the transmission of radio-frequency (RF) signals is a subject of considerable interest for future commercial and military systems [1]. So far, most effort has been done on intensity modulated analog optical links. However, the limitations of intensity modulated analog optical links on dynamic range are well-known [1]. In contrast, optical phase modulation has no fundamental limit to modulation depth besides that given by the available modulation range in optical phase modulators. However, since the traditional coherent receiver has the sinusoidal response limiting the overall dynamic range, the challenge to implement a linear phase modulated link lies in the receiver structure [3]. We have recently proposed, theoretically investigated, and experimentally demonstrated a novel coherent baseband (operation frequency: 0–2 GHz) optical phase-locked demodulator with feedback [4], [5]. We have experimentally shown that the proposed approach in [4] results in 15 dB of spurious-free dynamic range (SFDR) improvement compared to the traditional coherent receiver without the feedback. However, in order to operate the phase demodulator at high frequencies (>2 GHz), the baseband loop bandwidth would need to be very large to obtain a high degree of linearity. For instance, a loop operating at 20 GHz would require >100 GHz of loop bandwidth. This is far beyond feasible, considering the delay in the feedback loop and the challenges making electronics operate beyond 100 GHz. To overcome this problem, a novel approach using optical sampling at the demodulator is investigated. The basic idea is to use a pulsed laser source at the receiver unit (see Fig. 1). The received high-frequency input RF signal is, hence, sampled at a rate close to the pulsed laser source period. In this way, an intermediate frequency (IF) component is obtained that falls within the operating range of the baseband optical phase-demodulator. Using a detailed numerical model, we investigate how the signal-to-intermodulation ratio (SIR) of the demodulated optical signal is affected by the laser signal pulsewidth, loop gain, loop time-delay, input RF signal frequency, and timing and amplitude jitter of the pulsed optical source. The dynamical behavior of the sampling loop is compared to that of the baseband loop.

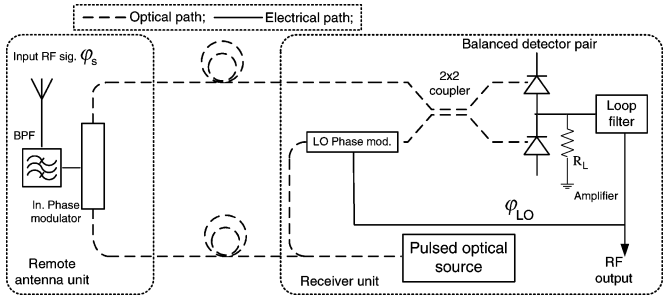

Fig. 1. General outline of phase-modulated optical link and phase-locked optical demodulator at the receiver unit.

II. Model Setup

The setup of the optical phase demodulator, using a sampling phase-locked loop (PLL), on which we base our model, is shown in Fig. 1. The received RF signal $\varphi_s(t)$ is used to directly modulate an input optical phase modulator at the remote antenna unit. The optical signal is then transported to the receiver unit where the optical signal phase $\varphi_s(t)$ is compared to the reference phase (signal) $\varphi_{\mathrm{LO}}(t)$ using the balanced detector pair with load resistance R_L. A single pulsed optical source is used for both the remote and the receiver unit. The signal from the balanced detector pair, containing the phase difference between $\varphi_s(t)$ and $\varphi_{\mathrm{LO}}(t)$, is then passed through the loop filter (low pass), amplified and applied to the LO phase-modulator. The original input RF signal $\varphi_s(t)$ is now, therefore, downconverted to an IF: $\omega_{\mathrm{IF}} = \omega_1 - \omega_{\mathrm{ls}}$. ω_1 is the frequency of the RF input signal and ω_{ls} is the repetition frequency of the pulsed optical source time-varying amplitude. The desired demodulated output RF signal $V_{\mathrm{out}}(t)$ is the electrical signal tapped before the LO

Manuscript received December 11, 2006; revised February 8, 2007. This material is based upon work supported by the Defense Advanced Research Projects Agency (DARPA) PHOR-FRONT Program under United States Air Force contract FA8750-05-C-0265.

The authors are with the Department of Electrical and Computer Engineering, University of California, Santa Barbara, CA 93106-9560 USA (e-mail: dz@com.dtu.dk).

Color versions of one or more of the figures in this letter are available online at http://ieeexplore.ieee.org.

Digital Object Identifier 10.1109/LPT.2007.895053

phase-modulator. Based on the model depicted in Fig. 1, a set of nonlinear differential equations describing total phase error $\varphi_e(t) = \varphi_s(t) - \varphi_{\rm LO}(t)$ and the output RF signal $V_{\rm out}(t)$ are derived. A detailed description of the baseband model is reported in [6]. For the sampling loop, the continuous-wave (CW) optical source is exchanged with the pulsed optical source and the rest of the equation system remains the same. We furthermore include the effect of timing and amplitude jitter associated with the optical pulse source. Timing jitter is modeled as Brownain motion phase error [2]. Amplitude jitter is modeled as colored noise where the power spectrum density (PSD) is phenomenologically described as $G(f) = \eta/(1 + (f/f_R)^2)$ [3], η is low-frequency jitter PSD, and f_R is the roll-off frequency. Loop gain is defined as $K = \pi P_{\rm ls}^{\rm av} A R_{\rm pd} R_L/(V_\pi \tau_{LF})$, where $P_{\rm ls}^{\rm av}$ is the average power of the pulsed optical source, A is the gain of the amplifier, $R_{\rm pd}$ is the responsivity of the photodiodes, R_L is the load resistance, and τ_{LF} is the inversely proportional to the bandwidth (BW) of loop filter. (V_π assumed equal for both phase modulators.) In order to characterize the SFDR of the system, the input RF signal is assumed to consist of two closely spaced frequencies: ω_1 and ω_2. The nonlinear response of the phase detector, pulsed optical source, etc., will result in intermodulation distortion of the demodulated signal. Third-order intermodulation products $\{2(\omega_1 - \omega_{\rm ls}) - (\omega_2 - \omega_{\rm ls}), 2(\omega_2 - \omega_{\rm ls}) - (\omega_1 - \omega_{\rm ls})\}$ fall at a frequency close to the demodulated signal and they cannot be filtered away, limiting the SFDR of the system [3]. The demodulated signal obtained by the sampling phase-locked optical demodulator is then characterized by the SIR which is the ratio between the power of the demodulated signal and the third-order intermodulation products. When the tracking LO phase-modulator nonlinearities are set to zero and assuming that the phase detection process is linear, $\sin[\varphi_e(t)] \approx \varphi_e(t)$, the total phase error for the (locked) baseband loop (CW optical source) including the loop filter becomes [6]

$$\varphi_e(t) = \frac{1}{K^2 + \omega_1^2}\left(M_{\rm in}\omega_1^2 \cos[\omega_1 t] - K \sin[\omega_1 t]\right) \quad (1)$$

where $M_{\rm in} = \pi V_1/V_\pi$. In (1), it is assumed for simplicity that the input RF signal consists of only one tone at frequency ω_1 with the amplitude V_1. Since there are no nonlinearities in the loop, $\varphi_e(t)$ contains only a frequency component at ω_1, as expected. Equation (1) also shows that as K approaches infinity, the total phase error $\varphi_e(t)$ approaches zero, i.e., the demodulated signal $V_{\rm out}(t)$ is a replica of a input RF signal. Under the same assumption as for the baseband loop, the total phase error for the sampling loop is governed by the following equation:

$$\varphi_e(t) = M_{\rm in} \cdot \left(\cos[\omega_1 t] - \frac{K \sin^3[\omega_1 t]}{6\omega_1} - \frac{A_0 K \sin[\omega_1 t] - \omega_1 t \cos[\omega_1 t]}{2\omega_1}\right) \cdot e^{-\frac{1}{2}\frac{A_0 K (\cos[\omega_1 t]\sin[\omega_1 t] - \omega_1 t)}{\omega_1}} \quad (2)$$

where we have assumed raised cosine pulse shape. A_0 is the amplitude of the pulses. It is observed in (2) that $\varphi_e(t)$ not only contains the frequency components at ω_1, but also the multiples of ω_1 (harmonics). The amplitude of harmonics increases as the loop gain is increased. This is in contrast with the baseband loop. Furthermore, by inspecting (2), we can qualitatively conclude that the amplitude of the harmonics can be reduced by increasing the frequency ω_1. In Section III, it is confirmed that the sampling induces extra nonlinearities in the overall loop response by using the time domain large signal numerical model based on nonlinear differential equations describing $\phi_e(t)$ and $V_{\rm out}(t)$.

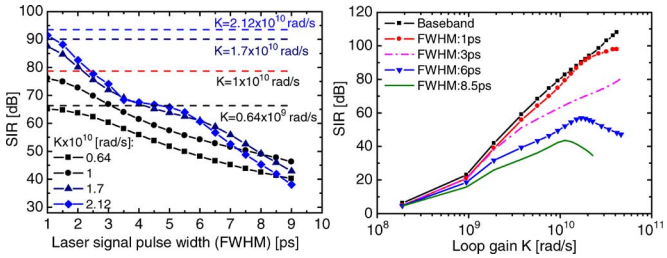

Fig. 2. (a) SIR as a function of pulsewidth (FWHM) of the laser signal for selected values of the loop gain. (b) SIR as a function of input signal frequency for selected values of the loop gain. Pulsewidth of the laser signal: 1 ps.

III. Sampling versus Baseband Loop

In this section, the linearity of the optical phase demodulator, based on sampling PLL, is investigated by computing the SIR of the demodulated signal. An input RF signal modulation depth of $\pi/2$ is assumed in all simulation results and the pulse shape of the optical pulse source is Gaussian. In Fig. 2(a), the SIR is computed as a function of the full-width at half-maximum (FWHM) of the pulsed optical source signal for selected values of K. The input RF signal frequencies are $\omega_1 = 20$ GHz + 0.9 GHz, $\omega_2 = 20$ GHz + 1.6 GHz, and $\omega_{\rm ls} = 20$ GHz. The down-converted IF components, at which the loop will operate, are $\omega_{{\rm IF},1} = \omega_1 - \omega_{\rm ls}$ and $\omega_{{\rm IF},2} = \omega_2 - \omega_{\rm ls}$. The constant lines correspond to the SIR obtained by the baseband loop for the corresponding values of the loop gain. For the baseband case, $\omega_1 = 0.9$ GHz and $\omega_2 = 1.6$ GHz. In general, Fig. 2(a) shows that the SIR decreases as the pulsewidth is increased and thereby indicates that the sampling induces a penalty in the SIR. This is in accordance with (2). However, it should be noted that for the open-loop sampling system, there is no degradation in the SIR as the pulsewidth is varied. Furthermore, we observe from Fig. 2(a) that as the pulsewidth is decreased, the SIR of the sampling loop approaches the value obtained by the baseband loop. However, very short pulses ($\sim$1 ps) are required in order to preserve the SIR. Fig. 2(a) furthermore indicates that for relatively high values of the pulsewidth, increasing K does not improve the SIR. We, therefore, need to investigate how the SIR of the demodulated signal is affected by increasing the loop gain. In Fig. 2(b), the SIR is computed as a function of the loop gain for different values of the pulsewidth. As a reference, we also plot the SIR obtained by the baseband loop in the same figure. Fig. 2(b) shows that for increasing loop gain and pulsewidth, the SIR of the demodulated signal, obtained by the sampling loop deviates from the SIR obtained by the baseband loop. The penalty in the SIR is increased as the loop gain is increased. This is in accordance with (2), as discussed earlier. However, the penalty decreases for decreasing pulsewidth. Fig. 2(b) also shows that the SIR is less sensitive to the pulsewidth for low values of the loop gain. Furthermore, the SIR curve starts to decrease, for the pulsewidth of 6 and 8.5 ps, as the loop gain is sufficiently increased. The value of the loop gain for which the

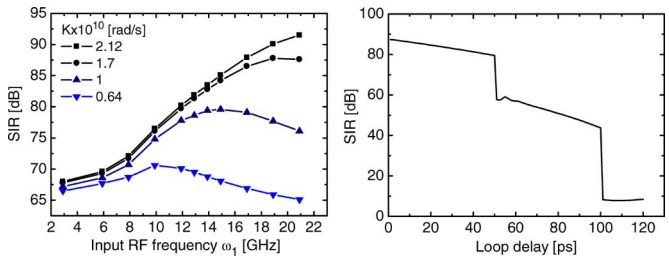

Fig. 3. (a) SIR as a function of loop gain K for selected values of the FWHM of the pulsed laser source. (b) SIR as a function of loop delay in a sampled second-order feedback loop with 20-GHz pulse rate and 1-GHz IF.

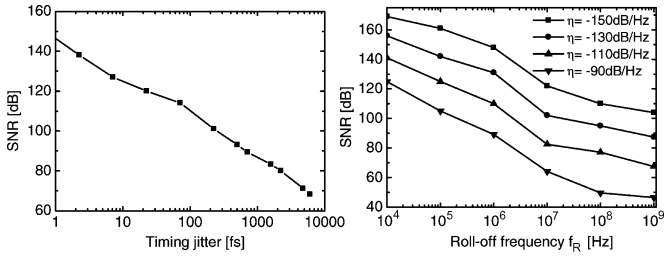

Fig. 4. SNR of the demodulated signal in 500-MHz BW. (a) SNR as a function of timing jitter of the pulsed source. Integration range: 100 Hz–10 GHz. (b) SNR as a function of roll-off frequency f_R when η is varied.

SIR starts to decrease, decreases with increasing pulsewidth. For the pulsewidth of 8.5-ps pulsewidth, the loop looses its lock if the loop gain is increased beyond 2.5×10^{10} rad/s. Next, it is investigated how SIR is affected by input RF signal frequency [Fig. 3(a)]. The pulsewidth is set to 1 ps. The frequency difference $\omega_1 - \omega_{\rm ls}$ and $\omega_2 - \omega_{\rm ls}$ is held constant and the sampling loop will, therefore, operate at a constant intermediate frequency. Fig. 3(a) indicates that for relatively high values of loop gain, 2.12×10^{10} and 1.17×10^{10} rad/s, the SIR of the demodulated signal increases as the input signal frequency is increased. For relatively low values of the input RF signal frequency, the dependence of the SIR on the loop gain is negligible. In that case, the SIR is limited by the nonlinearities of the low-frequency optical pulsed source. For the relatively low value of the loop gain $(K = 0.64 \times 10^{10}$ rad/s), the SIR does not seem to be much affected by increasing ω_1. Furthermore, for $K = 0.64 \times 10^{10}$ and 1×10^{10} rad/s, there is an optimal value of the input signal frequency for which the SIR is increased. So far, the effect of the finite delay in the loop has been considered to be small. In a baseband loop, the effect of loop delay is well known to limit the available loop gain, while maintaining stability [7]. The delay gets more significant the higher the frequency. In a sampled loop, the effective feedback delay is given by that of the pulse rate. No information can in this case be forwarded when no pulse is present in the loop, assuming the pulsewidth is narrower than the physical delay of the loop. In other words, the sampled loop will operate more efficiently at higher input frequencies. Fig. 3(b) shows the effect of a physical loop delay in a sampled loop. A 20-GHz pulse rate and 1-GHz IF has been assumed. Further, idealized delta pulses have been assumed to clearly isolate the impact of the loop delay. The performance degrades slowly with increasing delay up to the point where the delay exceeds the pulse repetition ratio, after which step degradation in performance occurs corresponding to a delayed feedback to the second proceeding pulse. It can be observed that the effect of loop delay is relatively weak compared to the pulse rate.

In Fig. 4(a), signal-to-noise ratio (SNR) of the demodulated signal is computed as a function of timing jitter of the pulsed source. As expected, the SNR decreases as the timing jitter increases. In Fig. 4(b), the effect of amplitude jitter on SNR is investigated. Even though η is relatively large, high values of SNR can be obtained by having low f_R.

IV. Conclusion

A novel approach of using optical sampling, in order to increase operation frequency of the optical phase demodulator, has been theoretically investigated. The optical sampling inherently induces a penalty in the SIR compared to the baseband loop. However, for very short pulsewidths (<2 ps) and high input signal frequencies, the penalty is very small making this technique promising for high-frequency analog optical links. From the practical point of view, one needs to deal with close path matching of very narrow pulses, close polarization matching, bandwidth limitations due to loop group delay, etc.

Acknowledgment

The authors would like to thank L. Coldren, L. Lembo, S. Pappert, and R. Smith for useful conversations and input.

References

[1] C. H. Cox, E. I. Ackerman, G. E. Bets, and J. L. Prince, "Limits on performance of RF-over-fibre links and their impact on device design," *IEEE Trans. Microw. Theory Tech.*, vol. 54, no. 2, pp. 906–920, Feb. 2006.

[2] A. Mehrotra, "Noise analysis of phase-locked loops," *IEEE Trans. Circuits Syst. I, Fundam. Theory. Appl.*, vol. 49, no. 9, pp. 1309–1316, Sep. 2002.

[3] R. F. Kalman, J. C. Fan, and L. G. Kazovsky, "Dynamic range of coherent analog fiber-optic links," *J. Lightw. Technol.*, vol. 12, no. 7, pp. 1263–1277, Jul. 1994.

[4] H. F. Chou, A. Ramaswamy, D. Zibar, L. A. Johansson, L. Coldren, and J. Bowers, "SFDR improvement of a coherent receiver using feedback," presented at the Proc. IEEE Conf. Coherent Optical Technologies and Applications (COTA), Whistler, Canada, 2006, Paper CFA3.

[5] D. Zibar, L. A. Johansson, H. F. Chou, A. Ramaswamy, and J. E. Bowers, "Time domain analysis of a novel phase-locked coherent optical demodulator," presented at the Proceeding of IEEE Conference on Coherent Optical Technologies and Applications (COTA), 2006, Paper JWB1.

[6] D. Zibar, L. A. Johansson, H. F. Chou, A. Ramaswamy, M. Rodwell, and J. E. Bowers, "Dynamic range enhancement of phase-modulated analog optical links," *Opt. Express*, vol. 15, no. 1, pp. 33–44, Jan. 2007.

[7] F. Gardner, *Phase Lock Techniques*, 3rd ed. New York: Wiley, 2004.